

Sonic Hedgehog Signaling Affected by Promoter Hypermethylation Induces Aberrant *Gli2* Expression in Spina Bifida

Xiao-Lin Lu¹ · Li Wang¹ · Shao-Yan Chang¹ · Shao-Fang Shangguan¹ · Zhen Wang¹ · Li-Hua Wu¹ · Ji-Zhen Zou² · Ping Xiao² · Rui Li¹ · Yi-Hua Bao¹ · Z-Y Qiu¹ · Ting Zhang¹

Received: 2 May 2015 / Accepted: 16 September 2015 / Published online: 7 October 2015
© Springer Science+Business Media New York 2015

Abstract GLI2 is a key mediator of the sonic hedgehog (Shh) signaling pathway and plays an important role in neural tube development during vertebrate embryogenesis; however, the role of *gli2* in human folate-related neural tube defects remains unclear. In this study, we compared methylation status and polymorphisms of *gli2* between spina bifida patients and a control group to explore the underlying mechanisms related to folate deficiency in spina bifida. No single nucleotide polymorphism was found to be significantly different between the two groups, although *gli2* methylation levels were significantly increased in spina bifida samples, accompanied by aberrant GLI2 expression. Moreover, a prominent negative correlation was found between the folate level in brain tissue and the *gli2* methylation status ($r=-0.41$, $P=0.014$), and *gli2* hypermethylation increased the risk of spina bifida with an odds ratio of 12.45 (95 % confidence interval: 2.71–57.22, $P=0.001$). In addition, we established a cell model to illustrate the effect of *gli2* expression and the accessibility of chromatin affected by methylation. High *gli2* and *gli1* mRNA expression was detected in 5-Aza-treated cells, while *gli2* hypermethylation

resulted in chromatin inaccessibility and a reduced association with nuclear proteins containing transcriptional factors. More meaningful to the pathway, the effect gene of the Shh pathway, *gli1*, was found to have a reduced level of expression along with a decreased expression of *gli2* in our cell model. Aberrant high methylation resulted in the low expression of *gli2* in spina bifida, which was affected by the change in chromatin status and the capacity of transcription factor binding.

Keywords *gli2* · Methylation · Sonic hedgehog pathway · Spina bifida

Introduction

Neural tube defects (NTDs) are severe malformations that occur during development of the central nervous system. A few key signaling pathways for NTDs have been identified, including noncanonical Wnt signaling (planar cell polarity), sonic hedgehog (Shh), and folate/1-methyl carbon metabolic pathway [1–5]. Though over 200 genes have been found to be involved in the regulation of neural tube closure in animal models, increasing attention is being focused on epigenetic mechanisms in NTDs [6–8].

Genetics and environmental factors are thought to be involved in NTD etiology. For instance, folate is integral to the intracellular one-carbon metabolism used in DNA methylation and a proportion of NTDs were shown to be prevented by folic acid supplementation [9]. Moreover, a study by Farkas et al. suggested that a gene–nutrition interaction between folate intake, DNA methylation alternations in folate transport genes, and genotypes partly accounted for NTD births [10]. We also observed aberrant DNA methylation in

Xiao-Lin Lu and Li Wang contributed equally to this work.

Electronic supplementary material The online version of this article (doi:10.1007/s12035-015-9447-0) contains supplementary material, which is available to authorized users.

- ✉ Li Wang
lily_wang@yeah.net
- ✉ Ting Zhang
zhangtingcv@126.com

¹ Beijing Municipal Key Laboratory of Child Development and Nutriomics, Capital Institute of Pediatrics, Beijing 100020, China

² Department of Pathology, Capital Institute of Pediatrics, Beijing 100020, China

human fetuses affected with NTDs in our previous studies [11, 12].

The Shh signal pathway guides pattern formation and cell fate in many structures during vertebrate embryogenesis, especially in neural tube development. In particular, it plays an important role in regulating neuronal differentiation along the dorsoventral axis of the neural tube through the SHH concentration gradient and is involved in the regionalization of the developing central nervous system, which begins at the neural plate stage [13, 14]. Previous studies have revealed that mutations of key Shh pathway genes cause ectopic neural tube development [4, 14, 15]. Furthermore, the aberrant methylation status of promoter regions in genes of the Shh pathway is found to be associated with certain nervous system defects [16, 17].

GLI family proteins, including GLI1, GLI2, and GLI3, are mediators of Shh signaling. GLI1 is a strong activator of target genes, while GLI3 has an inhibitory role in Shh signaling [18, 19]. GLI2 is thought to act as a transcriptional activator of Shh-responsive genes, such as *gli1*, and a number of independent studies have confirmed that GLI2 has the highest relative importance in certain ectopic states such as NTDs and tumors [15, 20]. Under the general consensus that folate-related metabolism is important in NTD development, we postulated that a link might exist between folate deficiency and Shh pathway-related NTDs via the aberrant methylation of *gli2*.

The present study therefore explored the possible mechanism of aberrant *gli2* function in spina bifida. We investigated the potential association between *gli2* single nucleotide polymorphisms (SNP) and the risk of spina bifida to determine its genetic cause. We compared the methylation status of the *gli2* promoter region and the area near the transcription start site (TSS), between spina bifida and control individuals. We also assessed the possible correlation among the folate level, *gli2* methylation status, and the occurrence of spina bifida. Additionally, we employed chromatin analysis and surface plasmon resonance (SPR) methods to detect the effect of methylation on the chromatin state and on the binding of nuclear extracts to DNA, respectively.

Materials and Methods

Sample Collection

All samples were obtained from a long-term surveillance program concerning the high prevalence of NTDs in the Lüliang Mountain area of northern China. Fetuses affected with NTDs were obtained from stillbirth deliveries and medical abortions based on a diagnosis using B-ultrasound. Definitive diagnosis was made by postmortem according to the International Classification of Disease, Tenth Revision, code Q05 spina bifida, Q00 anencephaly, and Q01 encephalocele. Control

samples were aborted for nonmedical reasons and were confirmed to have no deformities by postmortem. None of the pregnant women had received periconceptional folic acid supplementation. All participants provided their informed consent, and the study protocol was reviewed and approved by the Institutional Review Board of the Capital Institute of Pediatrics in Beijing, China. Detailed clinical and socioeconomic information was collected by local trained doctors.

A total of 251 samples were collected from July 2005 to August 2010 for *gli2* SNP analysis, including 113 controls and 138 subjects with NTDs from this surveillance program. Subject characteristics are shown in Supplementary Table 1. Among the NTD samples, 53 had spina bifida, 68 had anencephaly, and 17 had encephalocele. Fifty-two control samples and 70 subjects with spina bifida were used for methylation analysis, and the characteristics of these subjects are shown in Table 1.

Immunohistological Analyses

Immunohistochemical (IHC) staining was performed according to standard protocols using anti-GLI2 (AV31885, Sigma-

Table 1 Characteristics of participants in methylation analysis

	Controls (<i>n</i> =52) <i>n</i> (%) ^a	Cases (<i>n</i> =70) <i>n</i> (%) ^a	<i>P</i>
Mother's age (years) ^b	29.69±17.83	33.41±20.96	0.304
Education level of mother ^c			
<High school graduation	45(90.0)	56(82.4)	0.242
≥High school graduation	5(10.0)	12(17.6)	
Missing	2	2	
Gravidity (<i>n</i>) ^c			
Primigravida	17(32.7)	24(34.3)	0.854
Multigravida	35(67.3)	46(65.7)	
Missing		1	
Parity (<i>n</i>) ^c			
0	15(28.8)	23(33.3)	0.509
1	28(53.8)	30(43.5)	
≥2	9(17.3)	16(23.2)	
Missing		1	
Gestational week (weeks) ^c			
≤20	21(40.4)	23(32.9)	0.054
21~24	22(42.3)	21(30.0)	
≥25	9(17.3)	26(37.1)	
Sex of offspring ^c			
Male	16(30.8)	32(46.4)	0.082
Female	36(69.2)	37(53.6)	
Missing		1	

^a Percentages may not equal 100 because of rounding

^b Values were mean±SD, Student's *t* test was used to calculate the *P* values

^c χ^2 test was used to calculate *P* values

Aldrich, St. Louis, MO, USA; dilution 1:250), anti-GLI1 (ab134906, Abcam Inc., Cambridge, MA, USA; dilution 1:300), and anti-PTCH1 (ab53715, Abcam Inc.; dilution 1:100) antibodies. Individual 3- μm -thick sections of paraffin specimen from four spina bifida brain tissues samples and four control samples paired by tissue type were employed in this experiment. Sections were de-waxed, underwent antigen retrieval, and the endogenous peroxidase activity was blocked by incubation in 5 % H_2O_2 for 5 min. The blocks were then incubated with primary antibodies overnight at 4 °C according to the manufacturers' protocols.

Subsequently, slides were washed three times in phosphate-buffered saline (PBS) and incubated with the non-specific antibody at room temperature for 1 h. The slides were then rinsed, stained with 3,3-diaminobenzidine and hematoxylin, mounted, and visualized under a light microscope (model Eclipse 80i, Nikon, Tokyo, Japan).

The quantity and intensity of the positive cells were evaluated in 10 fields of view under a magnification of $\times 400$. Image-Pro Plus (IPP) 6.0 software was used to determine the percentage of positive cells in each image.

DNA Extraction and Bisulfite Treatment

Genomic DNA was extracted from 100-mg frozen brain or skin tissue using a standard phenol/chloroform extraction procedure, followed by ethanol precipitation. DNA with an OD260/OD280 absorbance ratio of 1.8–1.9 was used for subsequent work. A total of 200 ng genomic DNA from each brain tissue sample underwent bisulfite treatment using the EZ DNA methylation kit (Zymo Research, Irvine, CA, USA) according to the manufacturer's instruction. DNA from skin tissue was used to determine the genotype for SNP analysis.

Gli2 Methylation Analysis

The Sequenom MassARRAY platform (Sequenom, San Diego, CA, USA) was used to quantitatively analyze the methylation status of the region from -1000 bp to $+1000$ bp of the *gli2* TSS containing 49 potential CpG sites. According to the relative position of the TSS, the focus area was divided into Region_M1 and Region_M2. The system combined matrix-assisted laser desorption/ionization time-of-flight mass spectrometry and RNA base-specific cleavage was conducted as described in our previous study [11]. Polymerase chain reaction (PCR) primers were designed using the Sequenom epidesigner website (<http://epidesigner.com>). For each reverse primer, an additional T7 promoter tag for in vivo transcription was added, as well as a 10-mer tag on the forward primer to adjust for melting temperature differences (Supplementary Table 2). A total of 42 CpG sites (divided into 39 CpG units) were examined in this area, but 16 CpG sites

had no signal (Fig. 1). Spectra methylation ratios were generated by EpiTyper software version 1.0 (Sequenom).

Folate Analysis

The folate concentration of 11 control and 25 spina bifida brain tissue samples was determined using a competitive receptor binding immunoassay (Chemiluminescent Immunoenzyme Assay Access Immunoassay system II; Beckman Coulter, Krefeld, Germany).

All samples were measured using the same immunoassay batch. Briefly, 1.5-mg brain tissue was homogenized in Tris buffer and underwent nine cycles of 10-s sonication and 10-s ice incubation to increase the permeability of cell membranes. Sonication was performed using a compact ultrasonic device at 10 % power (model JY92-IIN, Scientz Biotechnology, Ningbo, China; 650 W, ultrasonic frequency 20 kHz). Next, the samples were centrifuged at 9000 g for 3 min at 4 °C to sediment insoluble material. The supernatant was used for folate determination in accordance with the manufacturer's instructions.

Because active calibration of the equipment is required every 28 days, Access Folate Calibrators (Chemiluminescent Immunoenzyme Assay Access Immunoassay system II; Beckman Coulter) were used to establish the calibration curve based on six folate levels: 0, and approximately 1.0, 2.5, 5.0, 10.0, and 20.0 ng/mL. Calibrators were run in duplicate. Before sample testing, quality control materials covering three levels of folate, QC1, QC2, and QC3 (BioRad Laboratories, Hercules, CA, USA), were determined to assure the validity of sample results.

Cell Culture

The human colorectal cancer HCT-15 cell line was obtained from the American Type Culture Collection (Manassas, VA, USA). Cells were cultured at 37 °C in a humidified 5 % CO_2 atmosphere in RPMI 1640 medium (Invitrogen, Carlsbad, CA, USA) supplemented with 10 % fetal bovine serum (GIBCO, Gaithersburg, MD, USA). Cells in the exponential growth phase were used for subsequent experiments.

For demethylation studies, cultured cells were incubated for 72 h in 0, 5, or 50 $\mu\text{mol/l}$ 5-Azacytidine (5-Aza; Sigma-Aldrich), a methylation inhibitor, and the medium was changed daily.

RNA Extraction and Reverse Transcription

Total RNA was extracted from cells using TRIzol Reagent (Invitrogen) according to the manufacturer's instructions. RNA concentration and purity were determined by the OD260/OD280 absorbance ratio. Reverse transcription was performed with the ProtoScript First Strand cDNA Synthesis

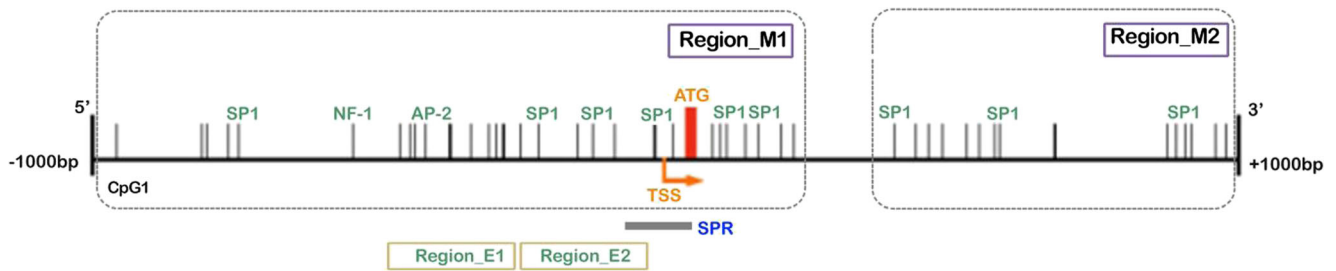


Fig. 1 Schematic representation of focused region surrounding *gli2* gene. The focused region, Region_M1 and Region_M2, spans positions –1000 to +1000 with respect to the transcription start site (TSS). There are 49 CpG sites in this region, depicted by vertical lines. Locations of putative transcription factor, such as Sp1, NF-1, and AP-2, are shown.

Kit (New England, Biolabs, Beverly, MA, USA) with oligo-dT, according to the instruction manual. cDNA was stored at –20 °C until required for use in real-time PCR.

Real-time PCR

To determine whether transcription of *gli2* and the activity of the Shh pathway were affected by methylation status, real-time PCR was carried out to compare the mRNA expression levels of *gli2*, *gli1*, and *ptch1* relative to the expression level of the housekeeping gene glyceraldehyde-3-phosphate dehydrogenase (*gapdh*). The primers were designed using Primer Express® software Version 3.0 (Applied Biosystems, Foster City, CA, USA). The following primers were used: *gli2* forward, 5'-CAC TCA AGG ATT CCT GCT CAT G-3' and reverse, 5'-TGC CAC TGA AGT TTT CCA GGA T-3'; *gli1* forward, 5'-CTA CAT CAA CTC CGG CCA AT-3', and reverse, 5'-CGG CTG ACA GTA TAG GCA GA-3'; *ptch1* forward, 5'-GGA TTC GAA GGT GGA AGT CA-3', and reverse, 5'-TCA AGC AGT TCT GGA AAG AGG-3'; *gapdh* forward, 5'-GAA GGT GAA GGT CGG AGT C-3', and reverse, 5'-GAA GAT GGT GAT GGG ATT TC-3'.

Briefly, quantitative analysis of cDNA was performed using a 7500 Fast Real-Time PCR system (Applied Biosystems) with SYBR Green PCR Master Mix (Applied Biosystems). Each PCR reaction consisted of 10- μ l 2 \times SYBR green master mixture, 0.5 μ l forward primer, 0.5 μ l reverse primer, 2 μ l cDNA template, and 7 μ l H₂O. Reactions were run in triplicate. Thermal cycling conditions were: 50 °C for 20 s, 95 °C for 10 min, then 40 cycles of 95 °C for 15 s, and 60 °C for 1 min. The expression levels of the target genes were calculated using the $2^{-\Delta\Delta C_t}$ method, for which, $\Delta C_t = C_{t_{\text{target}}} - C_{t_{\text{gapdh}}}$.

Chromatin Status Analysis

The EpiQ Chromatin Analysis Kit (Bio-Rad, Hercules, CA, USA) was used according to the manufacturer's instructions to determine if chromatin structure was quantitatively affected

by *gli2* methylation. This system used real-time PCR combined with in situ chromatin digestion and genomic DNA purification to quantify the *gli2* chromatin state in cultured cells. In this assay, heterochromatin was inaccessible to the nuclease, ensuring protection from nuclease digestion and accessibility for subsequent quantitative PCR.

HCT-15 cells grown in 48-well plates were treated with or without 50 μ mol/l 5-Aza for 3 days, in order to simulate the difference-methylation cell model. They were then divided into a digested group in which cells were treated with 100- μ l chromatin buffer containing 2 μ l nuclease and an undigested group treated with 100- μ l chromatin buffer only. All cells were incubated at 37 °C for 1 h, and 25 μ l EpiQ stop buffer (Bio-Rad, Hercules, CA, USA) was added for 10 min to suspend the digestion. Cells were then harvested and genomic DNA extracted according to the manufacturer's instructions for real-time PCR analysis. Two adjacent regions in the *gli2* promoter, Region_E1 and Region_E2, were randomly selected for this analysis. Primers were designed using the Primer3 website (<http://frodo.wi.mit.edu/primer3/>), as shown in Supplementary Table 2. The PCR cycling protocol was: 96 °C for 5 min, then 40 cycles of 95 °C for 15 s, 60 °C for 1 min, and 80 °C for 15 s. Samples were run in triplicate. The constitutively expressed *gapdh* and epigenetically silenced *rho* were used as the control gene (Con gene) and reference gene (Ref gene), respectively. The difference (ΔC_q) between nuclease-treated (digested) and untreated (undigested) samples was used to determine chromatin accessibility: chromatin accessibility = $(C_{t_{\text{Gli2_Digested}}} - C_{t_{\text{Gli2_Undigested}}}) / [(C_{t_{\text{Con_Digested}}} - C_{t_{\text{Con_Undigested}}}) - (C_{t_{\text{Ref_Digested}}} - C_{t_{\text{Ref_Undigested}}})]$. Each sample contained three biological replicates. Finally, the accessibility of chromatin in HCT-15 cells with and without 5-Aza treatment was compared.

Region_M1 and Region_M2 represent two regions, which are divided according to the relative position of the TSS. Region_E1 and Region_E2 indicate the two regions that have been randomly selected for chromatin status analysis. SPR indicates the region in which the SPR analysis was conducted

Surface Plasmon Resonance Analysis

Many transcription factors (TFs) were predicted to occur in the region focused on in this study, as shown by the Gene Regulation website (<http://www.gene-regulation.com/pub/>)

[programs/alibaba2/index.html](#)) (Fig. 1). We took advantage of the surface plasmon resonance-based (SPR-based) binding assay to validate the effect of methylation on the capacity of TF binding by comparing the affinity of methylated and nonmethylated DNA with nuclear extracts, which are rich in a variety of TFs.

HCT-15 cells in the exponential growth phase were harvested to obtain nuclear extracts using NE-PER Nuclear and Cytoplasmic Extraction Reagents according to the manufacturer's instructions (Thermo Fisher Scientific, San Diego, CA, USA). SPR analysis was carried out using the Biacore T100 system (GE Healthcare, Uppsala, Sweden). Biotinylated duplex oligonucleotide probes representing methylated and nonmethylated DNA were designed against a *gli2* sequence containing an SP1 binding site (sequences listed in Supplementary Table 2) and were immobilized on the streptavidin-modified surfaces of the different channels until saturation was reached to ensure identical surface density. Nuclear extracts from HCT-15 cells were diluted in NaCl buffer to 10 μ M before passing across the DNA-immobilized surfaces. All binding detections were performed using PBS with Tween as the running buffer at room temperature. Relative binding responses were determined by measuring changes in response unit (RU) values, before and after the passing of nuclear proteins. The results presented in the sensorgram were converted by BIA evaluation software. The experiment was performed in duplicate.

Single Nucleotide Polymorphism Selection and Detection

Tag SNPs in the promoter and full-length region of *gli2* were selected from the HapMap database, and exon SNPs were obtained from the NCBI SNP database. Primers were designed using Assay Designer 3.0 software for SNPs that had a minor allele frequency of no less than 0.10 in the Chinese Han population, reflecting the ethnicity of all samples, and were in strong linkage disequilibrium with other SNPs; r^2 was set to be no more than 0.80. PCR was used to amplify the polymorphic regions, and genotyping was undertaken using a MassARRAY platform by an experienced technician who was blinded to the diagnosis. To ensure the genotyping results, the negative controls were set and 60 % samples were re-genotyped. Subsequent genotype/allele frequency analyses were conducted for SNPs with a genotyping call rate greater than 90 %.

Statistical Analysis

Data were analyzed using SPSS 13.0 software (SPSS Inc.) and expressed as means \pm standard deviation. The means of two samples were compared using independent sample *t* tests, and the means of multiple samples were compared using

single factor analysis of variance. Odds ratios (ORs), which were used to evaluate the incidence of spina bifida relative to the methylation level, were calculated with 95 % confidence intervals (CIs). Adjusted ORs were calculated by logistic regression. Correlation analysis was performed using bivariate correlations. All *P* values were two-sided, and $P < 0.05$ was considered to be significant.

Results

GLI2 Protein Expression Was Significantly Decreased in Spina Bifida Brain Tissues

The expression level of GLI2 protein between case and control groups was assessed using IHC. As shown in Fig. 2b, the percentage of GLI2-positive cells in the spina bifida group was significantly reduced compared to that in normal fetus brain tissue ($P = 0.000$).

gli2 hypermethylation Was Associated with a High Occurrence of Spina Bifida

We compared the methylation status GLI2-encoding gene, *gli2*, in spina bifida samples with those of controls, as shown in Fig. 3a. The overall average (Global) *gli2* methylation level in the spina bifida group (67.70 %) was significantly higher than that in the control group (62.81 %) ($P = 0.000$), and this was observed for both Region_M1 and Region_M2. Spina bifida samples exhibited significantly higher DNA methylation levels (58.90 %) than control samples (53.77 %) ($P = 0.000$) in Region_M1 located around the TSS, whereas no significant difference in methylation level between the two groups was seen in Region_M2, located further away from the TSS relative to Region_M1. This suggests that the observed methylation difference in Region_M1 is probably the main contributor to the overall methylation trend.

In Region_M1, methylation at almost every CpG sites/unit in spina bifida samples was significantly higher than that in control samples. However, this trend was not observed in Region_M2, with the exception of the CpG46 site (Fig. 3b).

Logistic analysis then was conducted to assess the risk of spina bifida with aberrant methylation levels in *gli2*. Spina bifida samples were divided according to control sample methylation level quartiles (Table 2). With regard to the overall average (Global) *gli2* methylation level, especially Region_M1, more than half of spina bifida samples (57.1 and 64.3 %, respectively) were grouped into the highest quartile (methylation level ≥ 65.75 and 57.01 %, respectively). However, in Region_M2, only 20.0 % of spina bifida samples were in this same quartile

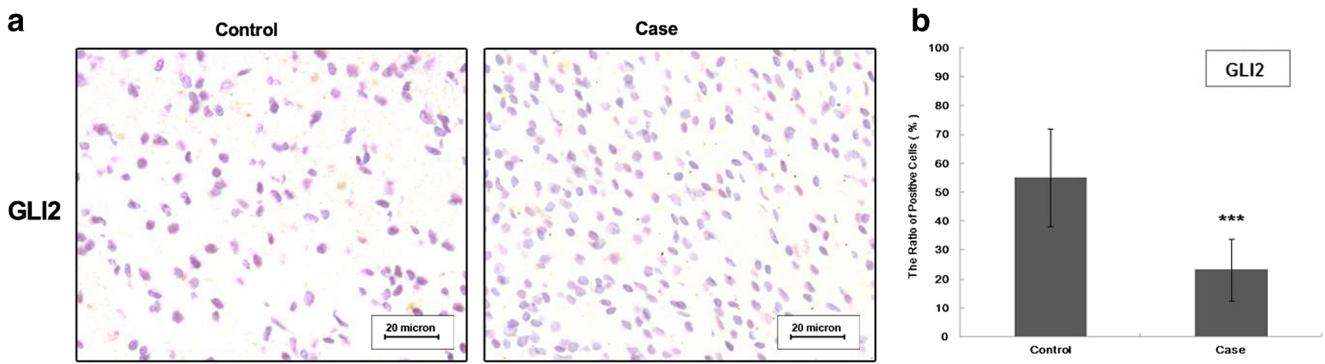


Fig. 2 Immunostaining of GLI2 in brain tissue of samples isolated from patients with spina bifida or controls. **a.** Blue color indicated cells, with negative staining; brown color indicated the immunoreactivity. **b.** The

ratio of GLI2-positive cells in spina bifida samples was significantly lower than that in controls. Results were shown as mean±SD. ****P*<0.001

(methylation level ≥87.55 %). High methylation levels in both Global and Region_M1 increased the risk of spina bifida by more than tenfold compared with low methylation levels (OR: 12.45, 95 % CI: 2.71–57.22 for Global; OR: 13.61, 95 % CI: 2.45–75.49 for Region_M1).

Brain Tissue Folate Levels Were Significantly Negatively Associated with *gli2* Methylation

We observed significantly higher folate levels in the brain tissue of 11 control group samples compared with 25 samples

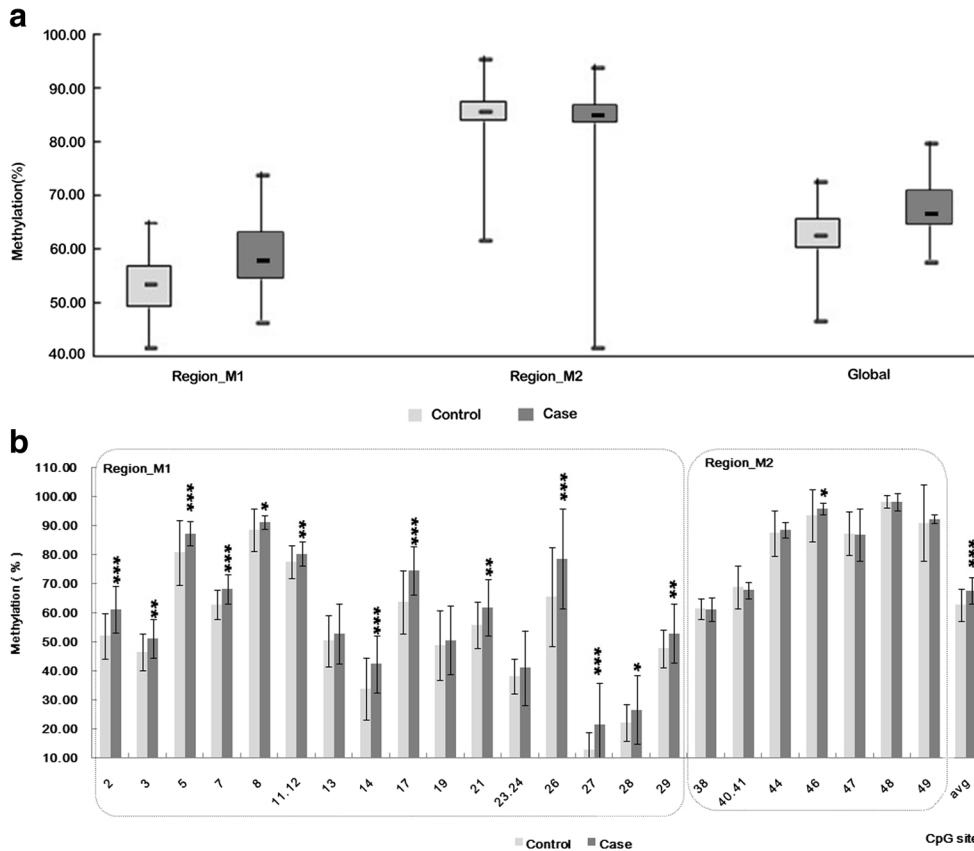


Fig. 3 The methylation level of the *gli2* gene in spina bifida group was significantly higher than that in control group. **a.** The average of methylation levels in the spina bifida group and control group. Boxes extend from the 25th to 75th percentiles and were divided by a solid line representing the median of each group. Whiskers extend from the minimum to maximum. In global, especially Region_M1, the difference of mean DNA methylation levels between two groups were statistically significant, the methylation level (mean, range) in control group and in case group are 53.80, 41.94–65.19, and 58.40, 46.75–74.30, in Region_

M1 and 63.00, 47.00–73.00, and 67.00, 58.00–80.00, globally, respectively (*P*<0.001 both, Student’s *t* test). **b.** Methylation level of specific CpG site in *gli2* gene. In Region_M1 region, the methylation levels of all 16 CpG sites/units in spina bifida group were significantly higher when compared with controls, except for the CpG13 and CpG23.24 sites. In Region_M2 region, only one CpG site, CpG 46, showed a significant difference in the methylation level between the two groups. Data are expressed as mean±SD. **P*<0.05, ***P*<0.01, ****P*<0.001

Table 2 Risk of spina bifida associated with methylation level of the specific region of *gli2* gene^a

	Controls n(%)	Cases n(%)	Adjusted OR(95 % CI) ^b	Adjusted P
Region_M1				
≤P25[n(%)]	10(19.2)	2(2.9)	1	
P25~P75[n(%)]	29(55.8)	23(32.9)	3.96(0.75–20.98)	0.106
≥P75[n(%)]	13(25.0)	45(64.3)	13.61(2.45–75.49)	0.003
Region_M2				
≤P25[n(%)]	14(26.9)	18(25.7)	1	
P25~P75[n(%)]	25(48.1)	38(54.3)	1.09(0.44–2.68)	0.847
≥P75[n(%)]	13(25.0)	14(20.0)	0.86(0.29–2.54)	0.783
Global				
≤P25[n(%)]	13(25.0)	3(4.3)	1	-
P25~P75[n(%)]	28(53.8)	27(38.6)	3.77(0.93–15.29)	0.063
≥P75[n(%)]	11(21.2)	40(57.1)	12.45(2.71–57.22)	0.001

OR odds ratio

^a Cutoffs defined as 25th and 75th percentiles of the control group methylation level^b Adjusted by gestation week and sex by logistic regression

from the spina bifida group (0.29 ± 0.03 nmol/L vs 0.17 ± 0.07 nmol/L, respectively, $P=0.000$) (Fig. 4a). We also analyzed the correlation between *gli2* methylation and folate levels of brain tissue to investigate the possible effect of folate deficiency on the *gli2* methylation status. As shown in Fig. 4b, the methylation level of Region_M1 and the overall average (Global) *gli2* methylation level had significant negative correlation with the folate levels of brain tissue.

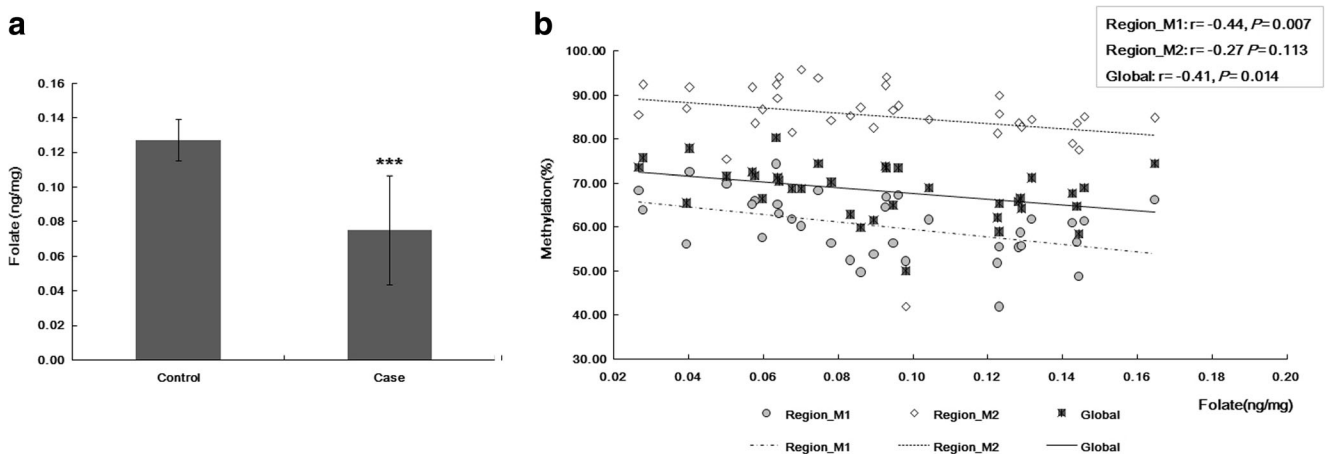


Fig. 4 Correlation between folate levels in the brain tissue and methylation status in *gli2* gene. Folate concentrations of the brain tissue were analyzed in 36 samples, including 11 controls and 25 spina bifida. **a.** Folate level in spina bifida samples was significantly lower than that in control samples. Data are expressed as mean±SD. *** $P<0.001$. **b.** The

Gli2 Transcription Was Significantly Negatively Correlated with its Methylation Level

Next, we established a methylation model using 5-Aza to alter the methylation status of *gli2* in HCT-15 cells to explore whether *gli2* transcription was affected by altered methylation. As shown in Fig. 5a, *gli2* methylation levels were significantly reduced in both groups of HCT-15 cells treated with 5-Aza (at 5 and 50 $\mu\text{mol}/\mu\text{l}$). Accordingly, the transcription of *gli2* was significantly increased in treated groups compared with the untreated group. In particular, the transcription level of *gli2* in the group of cells treated with the higher concentration of 5-Aza (50 $\mu\text{mol}/\mu\text{l}$) was significantly higher than that of cells in the lower concentration-treated group (5 $\mu\text{mol}/\mu\text{l}$), though no significant difference in methylation between the two groups was recorded. This implies that *gli2* transcription is sensitive to changes in DNA methylation, perhaps particularly in the Region_M1 (Fig. 5b). Moreover, the transcription of *gli2* was significantly negatively correlated with its methylation level, suggesting that aberrantly high methylation leads to the repression of *gli2* transcription (Fig. 5c).

Chromatin Accessibility and Nuclear Extract Binding Were Influenced by the Altered *gli2* Methylation Status

To further investigate the possible mechanism underlying changes in transcription activity based on methylation status, EpiQ chromatin analysis was used to monitor chromatin accessibility. This methylation diversity model was constructed in HCT-15 cells treated with 5-Aza. The analysis of chromatin status was carried out in two adjacent regions, Region_E1 and Region_E2. As shown in Fig. 6a, the methylation level in the

abscissa represented the concentration of brain tissue folate. The ordinate was the ratio of methylation of each sample in Region_M1, Region_M2, and Global. The folate level had a significant negative correlation with the *gli2* methylation level in Region_M1 and Global

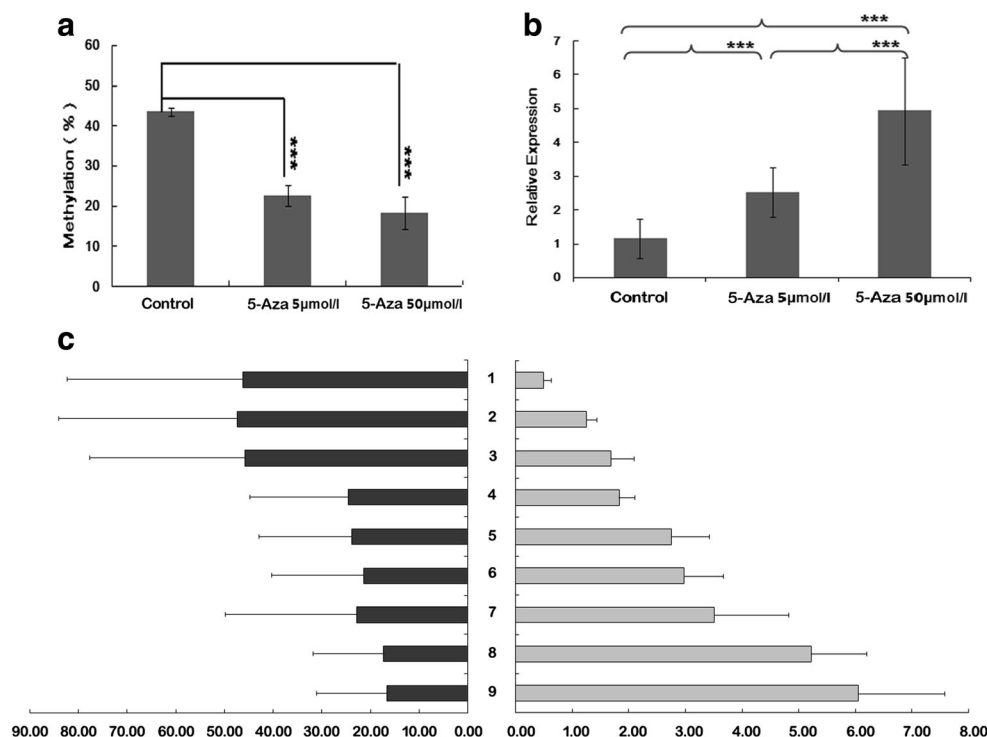


Fig. 5 The mRNA expression of *gli2* gene was associated with its methylation level in the region around TSS. Data are shown as mean \pm SD. *** $P < 0.001$. Cells were treated with 0 (lines 1–3), 15 (lines 4–6), or 50 μm (lines 7–9) 5-Aza and assayed for *gli2* expression using real-time PCR and the level of methylation. **a.** The higher the concentration 5-Aza treated, the lower the methylation level that was found. **b.** mRNA expression of *gli2* gene was examined. The value was defined as

expression ratio of *gli2* to *gapdh*. Higher expression of *gli2* gene appeared in 5-Aza-treated groups when compared with control group, which was not treated with 5-Aza. **c.** Expression of *gli2* gene was significantly negatively correlated with the global methylation level, $r = -0.70$. The left bar stood for the methylation level, but the right bar stood for the transcription level of *gli2* gene

region including Region_E1 and Region_E2 was significantly decreased by treatment with 5-Aza. Subsequently, in both regions, chromatin accessibility in the treated group was almost twice as high as that in the untreated group, suggesting that a tighter and more inaccessible chromatin status results from a higher methylation level (Fig. 6b).

TF binding is thought to be affected by chromatin status, so we next used SPR to investigate TF binding possibly affected by *gli2* methylation status. Using bioinformatic analysis, we inferred that the transcription factor SP1 could bind to the region of *gli2* shown to have an obvious methylation difference. Negative RU values were detected in two repeat experiments, indicating that nonmethylated DNA was associated with more nuclear proteins, containing SP1, than hypermethylated DNA (Fig. 6c). This suggested that *gli2* transcription would partially be influenced by methylation as a result of altered TF binding.

High *gli1* Expression Was Observed in Association with Low *gli2* Methylation, Suggesting that the Shh Pathway Might be Inhibited by *gli2* Hypermethylation

It is widely believed that GLI1 is an indicator of Shh pathway activity, and *ptch1* is the downstream target gene of GLI1 and key mediator of Shh pathway [17]. The expression of the target

genes, *gli1* and *ptch1*, was analyzed to evaluate possible changes in Shh pathway activity with an aberrant *gli2* expression. Consistent with the outcome from our GLI2 expression analysis (Fig. 2), IHC analysis of brain tissue revealed that GLI1 was expressed at lower levels in spina bifida samples than that in control samples, and that PTCH1 expression was higher in the spina bifida group, although neither difference was significant (Fig. 7a). Similarly, differences in mRNA expression of the homologous gene in the HCT-15 cell model were almost in agreement with in vivo findings, in that *gli1* expression was the greatest in cells treated with the highest concentration of 5-Aza, in which *gli2* also demonstrated the highest transcription level. However, the transcription level of *ptch1* in 5-Aza-treated cells was significantly lower than in the untreated group (Fig. 7b).

gli2 SNP Distribution did not Differ Between Spina Bifida and Control Samples

A total of 22 *gli2* SNPs, including seven exonic SNPs and 15 tag SNPs, were compared between the control and NTD groups, especially the spina bifida subtype of the NTD group. Only the homozygous mutation AA of SNP rs11681811, an intronic *gli2* SNP, showed a significantly higher frequency in the NTD group than the control group ($P = 0.033$), though the difference was not

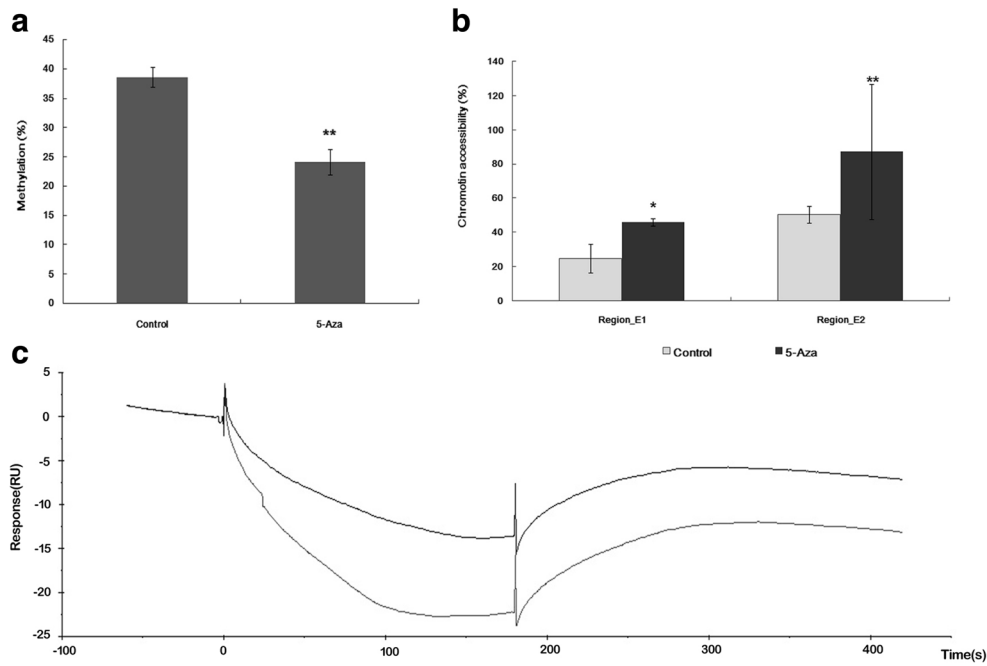
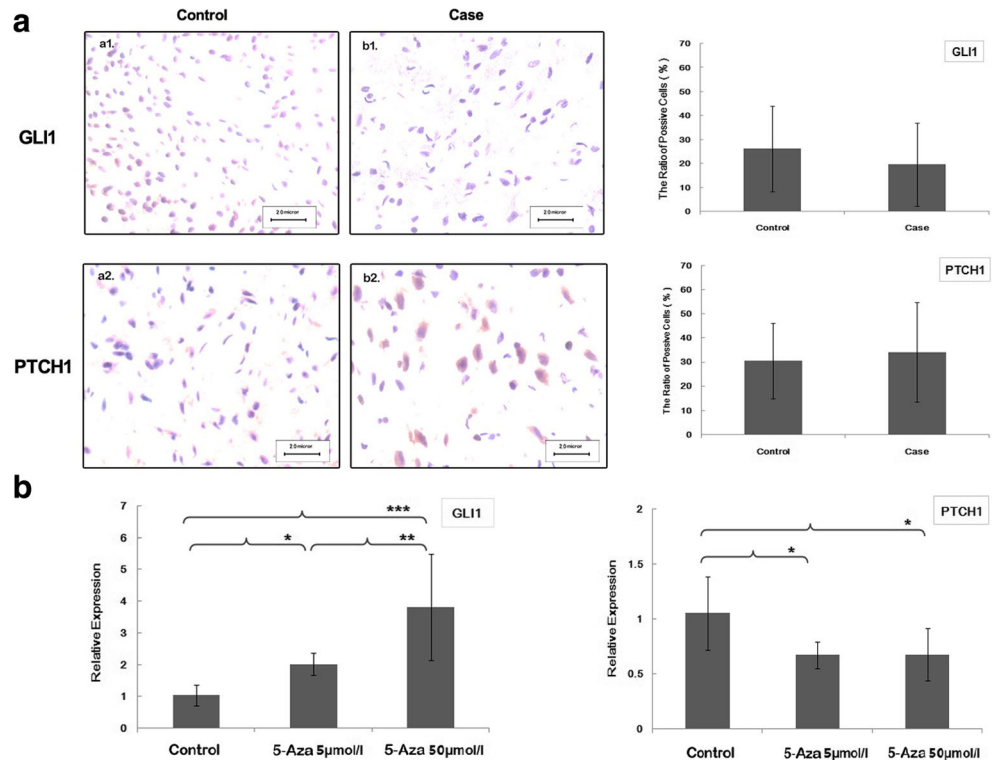


Fig. 6 Accessibility of chromatin and the binding affinity with nuclear extracts were related to hypermethylation in *gli2* gene. **a.** Methylation level in HCT15 cells treated with 5-Aza were significantly lower when compared with untreated control. The actual measurements of two groups, mean±SD, were 24.07±2.15 and 38.53±1.70, respectively. **b.** Accessibility of chromatin in 5-Aza group was significantly higher than that in untreated group in two randomly selected regions from Region_

M1. Each value represents mean±SD of three experiments, and each experiment was performed in triplicate. **c.** SPR analysis showed that the binding affinity with nuclear extracts was inhibited by DNA methylation. SPR assay were performed twice. Response unit (RU)=RU_{Methylated}–RU_{nonmethylated}. Negative RU value indicated that nonmethylation DNA chain integrates more nuclear proteins than methylation DNA. **P*<0.05, ***P*<0.01

Fig. 7 The mRNA expression between groups of *gli1* had the same trend as *gli2*, but *ptch1* was on the opposite of GLI2. **a.** Immunostaining of GLI1 and PTCH1 in the brain tissue from spina bifida and control samples. *a1* and *a2* were from control samples; *b1* and *b2* were from spina bifida samples. Blue color indicated cells with negative staining; brown color indicated the immunoreactivity. The ratio of GLI1-positive cells in the spina bifida group was lower than that in control group, while the opposite was observed for PTCH1 expression between two groups. **b.** Relative mRNA level of *gli1* in HCT15 cells had the same trend with *gli2*, with the highest expression seen in 5-Aza 50 μmol/l group. However, another gene regulated by *gli2*, *ptch1*, had the inverse trend compared with *gli1* and *gli2*. Data are expressed as mean±SD. **P*<0.05, ***P*<0.01, ****P*<0.001



seen between the spina bifida group and the control group (Supplementary Table 3). Following stratification analysis according to gender, no significant differences in polymorphism frequency were found between the NTD and control groups in both male and female samples (data not shown).

Discussion

It is well known that aberrations of DNA methylation in genes belonging to the Shh signaling pathway are involved in dysplasia of the nervous system [16, 17]. In the present study, we evaluated the methylation status and SNP distribution of *gli2* to understand the observed aberrant low level of GLI2 expression in the brain tissue of spina bifida and to explore the underlying events leading to NTD development. Our results establish that *gli2* methylation levels are remarkably higher in the brain tissue of clinical spina bifida samples compared with that in controls, which is important because hypermethylation has been shown to suppress *gli2* expression.

Gene promoter regions are typically thought to be most sensitive to DNA methylation modification than the coding regions. Our results indicated that methylation levels of both case and control groups were lower in Region_M1, which encompasses the promoter region and TSS of *gli2*, than that in Region_M2. Additionally, methylation levels in Region_M1 were significantly higher in spina bifida samples compared with controls but this difference was not observed in Region_M2, suggesting that the notable difference in global methylation levels of *gli2* was mainly the attributes of the difference in the promoter region and area surrounding the TSS.

Folate is known to be an essential environmental factor for DNA methylation, and previous researches have identified a link between folate deprivation and induced aberrant one-carbon metabolism in NTDs [21, 22]. The association analysis of the current study showed that brain tissue folate levels were negatively associated with *gli2* methylation. Combined with the association analysis findings that the aberrant elevated methylation level of *gli2*, especially in Region_M1, was significantly positively associated with an increased risk of spina bifida, we propose that folate deprivation-related hypermethylation of the *gli2* promoter is a potential risk factor of spina bifida.

To elucidate the role of *gli2* methylation alteration in spina bifida, we constructed a methylation model using HCT-15 cells treated with 5-Aza in three different concentrations to investigate how *gli2* expression was affected by hypermethylation. We focused on Region_M1 because CpG sequences near the TSS were previously shown to be the best targets for gene silencing [23] and because the association between *gli2* hypermethylation and an increased risk of spina bifida was identified in Region_M1 not Region_M2. Our results show that methylation levels of *gli2* were negatively correlated

with its transcription level, suggesting an essential role for methylation in regulating *gli2* mRNA expression.

GLI2 contributes to the induction of the most ventral region of the neural tube, although the mechanism underlying the regulation of GLI2 activity remains to be determined [24, 25]. The expression of GLI2 was previously observed throughout the neural plate just before neural tube closure [26], while the development of the floor plate and adjacent ventral interneurons was severely affected in the spinal cord of mice lacking *gli2* [24]. Pan et al. mutated the mouse *gli2* allele in protein kinase A sites essential for *gli2* function, causing NTD phenotypes [15]. Taking all these findings into account, we speculate that the epigenetic silencing of *gli2* by hypermethylation is an important early event in the course of incomplete closure of the neural tube. GLI2 functions downstream of the Shh pathway and targets *gli1* and *ptch1*, and a high level of GLI protein expression is often indicative of activated Shh signaling [27]. The present results found that inhibition of *gli2* expression was accompanied by the decreased expression of *gli1* but not *ptch1*, which is considered to be a repressor of the Shh pathway. This indicates that the Shh pathway is suppressed in the brain tissue of embryos affected with spina bifida.

DNA methylation is involved in the regulation of gene transcription through its negative effect on transcription factor–DNA interactions and its attraction of methyl–CpG-binding proteins; it was also shown to influence chromatin structure [28]. Moreover, hypermethylation is necessary to maintain the status of heterochromatin, which is transcriptionally inactive [1, 29]. In our study, the observed reduced methylation in the 5-Aza-treated group of HCT-15 cells was associated with higher chromatin accessibility and increased *gli2* expression, suggesting that regulation of the chromatin status is the mechanism by which *gli2* transcription is affected by DNA methylation. Open and accessible chromatin was shown to be more likely to attract the binding of TFs [30, 31]. Our SPR assay findings agreed with these results because nonmethylated DNA were found to bind more nuclear extracts, which contained transcription factor SP1. Hypermethylation was previously shown to reduce the affinity of SP1 in its role as a transcriptional activator, ultimately leading to the inhibition of transcription [32, 33].

Some SNPs are known to increase the risk of NTD development [34, 35]. For example, Carter et al. found that a *gli2* variant was associated with gene expression in cases of anorectal atresia, which is another serious birth defect [36]. However, in our present study, no *gli2* SNPs were significantly associated with spina bifida, suggesting that epigenetic modifications rather than genetic factors of *gli2* are the primary mechanism responsible for spina bifida.

In conclusion, our data indicate that the epigenetic silencing of *gli2* by hypermethylation may be an important event in the development of spina bifida during embryogenesis. Our results suggest, for the first time, that a relationship exists between lower brain tissue folate levels and spina bifida via *gli2* methylation

modification. It appears that the chromatin status and TF binding capacity were interrupted by aberrant methylation and jointly suppressed *gli2* expression, resulting in the observed decreased activity of the Shh pathway. Hypermethylation of *gli2* is therefore a potential epigenetic mechanism related to the etiology of spina bifida.

Acknowledgments This project was supported by the National Natural Science Foundation of China (grant numbers 81370967 and 81270699) and Beijing Natural Science Foundation (7132036).

Conflicts of Interest None of the authors declared any conflict of interest.

References

- Sugimura K, Fukushima Y, Ishida M, Ito S, Nakamura M, Mori Y, Okumura K (2010) Cell cycle-dependent accumulation of histone H3.3 and euchromatic histone modifications in pericentromeric heterochromatin in response to a decrease in DNA methylation levels. *Exp Cell Res* 316(17):2731–2746
- Juriloff DM, Harris MJ (2012) A consideration of the evidence that genetic defects in planar cell polarity contribute to the etiology of human neural tube defects. *Birth Defects Res A Clin Mol Teratol* 94(10):824–840
- Matise MP (2013) Molecular genetic control of cell patterning and fate determination in the developing ventral spinal cord. *Wiley Interdiscip Rev Dev Biol* 2(3):419–425
- Murdoch JN, Copp AJ (2010) The relationship between sonic hedgehog signaling, cilia, and neural tube defects. *Birth Defects Res A Clin Mol Teratol* 88(8):633–652
- Beaudin AE, Stover PJ (2009) Insights into metabolic mechanisms underlying folate-responsive neural tube defects: a minireview. *Birth Defects Res A Clin Mol Teratol* 85(4):274–284
- Greene ND, Stanier P, Copp AJ (2009) Genetics of human neural tube defects. *Hum Mol Genet* 18(R2):R113–R129
- Wallingford JB, Niswander LA, Shaw GM, Finnell RH (2013) The continuing challenge of understanding, preventing, and treating neural tube defects. *Science* 339(6123):1222002
- Detrait ER, George TM, Etchevers HC, Gilbert JR, Vekemans M, Speer MC (2005) Human neural tube defects: developmental biology, epidemiology, and genetics. *Neurotoxicol Teratol* 27(3):515–524
- Greene ND, Stanier P, Moore GE (2011) The emerging role of epigenetic mechanisms in the etiology of neural tube defects. *Epigenetics* 6(7):875–883
- Farkas SA, Bottiger AK, Isaksson HS, Finnell RH, Ren A, Nilsson TK (2013) Epigenetic alterations in folate transport genes in placental tissue from fetuses with neural tube defects and in leukocytes from subjects with hyperhomocysteinemia. *Epigenetics* 8(3):303–316
- Wang L, Wang F, Guan J, Le J, Wu L, Zou J, Zhao H, Pei L (2010) Relation between hypomethylation of long interspersed nucleotide elements and risk of neural tube defects. *Am J Clin Nutr* 91(5):1359–1367
- Wu L, Wang L, Shangguan S, Chang S, Wang Z, Lu X, Zhang Q, Wang J et al (2013) Altered methylation of IGF2 DMR0 is associated with neural tube defects. *Mol Cell Biochem* 380(1–2):33–42
- Ybot-Gonzalez P, Cogram P, Gerrelli D, Copp AJ (2002) Sonic hedgehog and the molecular regulation of mouse neural tube closure. *Development* 129(10):2507–2517
- Yu K, McGlynn S, Matise MP (2013) Floor plate-derived sonic hedgehog regulates glial and ependymal cell fates in the developing spinal cord. *Development* 140(7):1594–1604
- Pan Y, Wang C, Wang B (2009) Phosphorylation of Gli2 by protein kinase A is required for Gli2 processing and degradation and the sonic hedgehog-regulated mouse development. *Dev Biol* 326(1):177–189
- Diede SJ, Guenthoer J, Geng LN, Mahoney SE, Marotta M, Olson JM, Tanaka H, Tapscott SJ (2010) DNA methylation of developmental genes in pediatric medulloblastomas identified by denaturation analysis of methylation differences. *Proc Natl Acad Sci U S A* 107(1):234–239
- Shahi MH, Afzal M, Sinha S, Eberhart CG, Rey JA, Fan X, Castresana JS (2010) Regulation of sonic hedgehog–GLI1 downstream target genes PTCH1, Cyclin D2, Plakoglobin, PAX6 and NKX2.2 and their epigenetic status in medulloblastoma and astrocytoma. *BMC Cancer* 10:614
- Li J, Wang C, Pan Y, Bai Z, Wang B (2011) Increased proteolytic processing of full-length gli2 transcription factor reduces the hedgehog pathway activity in vivo. *Dev Dyn* 240(4):766–774
- Karlstrom RO, Tyurina OV, Kawakami A, Nishioka N, Talbot WS, Sasaki H, Schier AF (2003) Genetic analysis of zebrafish *gli1* and *gli2* reveals divergent requirements for gli genes in vertebrate development. *Development* 130(8):1549–1564
- Nagao H, Ijiri K, Hirotsu M, Ishidou Y, Yamamoto T, Nagano S, Takizawa T, Nakashima K et al (2011) Role of GLI2 in the growth of human osteosarcoma. *J Pathol* 224(2):169–179
- Chandler AL, Hobbs CA, Mosley BS, Berry RJ, Canfield MA, Qi YP, Siega-Riz AM, Shaw GM (2012) Neural tube defects and maternal intake of micronutrients related to one-carbon metabolism or antioxidant activity. *Birth Defects Res A Clin Mol Teratol* 94(11):864–874
- Stover PJ (2009) One-carbon metabolism-genome interactions in folate-associated pathologies. *J Nutr* 139(12):2402–2405
- Hoffman AR, Hu JF (2006) Directing DNA methylation to inhibit gene expression. *Cell Mol Neurobiol* 26(4–6):425–438
- Jacob J, Briscoe J (2003) Gli proteins and the control of spinal-cord patterning. *EMBO Rep* 4(8):761–765
- Litingtung Y, Chiang C (2000) Control of Shh activity and signaling in the neural tube. *Dev Dyn* 219(2):143–154
- Hui CC, Slusarski D, Platt KA, Holmgren R, Joyner AL (1994) Expression of three mouse homologs of the *Drosophila* segment polarity gene *cubitus interruptus*, *Gli*, *Gli-2*, and *Gli-3*, in ectoderm- and mesoderm-derived tissues suggests multiple roles during postimplantation development. *Dev Biol* 162(2):402–413
- Shahi MH, Holt R, Rebhun RB (2014) Blocking signaling at the level of GLI regulates downstream gene expression and inhibits proliferation of canine osteosarcoma cells. *PLoS One* 9(5):e96593
- Reddington JP, Pennings S, Meehan RR (2013) Non-canonical functions of the DNA methylome in gene regulation. *Biochem J* 451(1):13–23
- Black JC, Whetstone JR (2011) Chromatin landscape: methylation beyond transcription. *Epigenetics* 6(1):9–15
- Razin SV, Iarovaia OV, Sjakste N, Sjakste T, Bagdoniene L, Rynditch AV, Eivazova ER, Lipinski M et al (2007) Chromatin domains and regulation of transcription. *J Mol Biol* 369(3):597–607
- Vassetzky Y, Lemaitre JM, Mechali M (2000) Specification of chromatin domains and regulation of replication and transcription during development. *Crit Rev Eukaryot Gene Expr* 10(1):31–38
- Kyo S, Takakura M, Fujiwara T, Inoue M (2008) Understanding and exploiting hTERT promoter regulation for diagnosis and treatment of human cancers. *Cancer Sci* 99(8):1528–1538
- Rhodes K, Rippe RA, Umezawa A, Nehls M, Brenner DA, Breindl M (1994) DNA methylation represses the murine alpha 1(I)

- collagen promoter by an indirect mechanism. *Mol Cell Biol* 14(9): 5950–5960
34. Knight JC (2003) Functional implications of genetic variation in non-coding DNA for disease susceptibility and gene regulation. *Clin Sci (Lond)* 104(5):493–501
 35. Molloy AM, Brody LC, Mills JL, Scott JM, Kirke PN (2009) The search for genetic polymorphisms in the homocysteine/folate pathway that contribute to the etiology of human neural tube defects. *Birth Defects Res A Clin Mol Teratol* 85(4):285–294
 36. Carter TC, Kay DM, Browne ML, Liu A, Romitti PA, Kuehn D, Conley MR, Caggana M et al (2013) Anorectal atresia and variants at predicted regulatory sites in candidate genes. *Ann Hum Genet* 77(1):31–46